A COMPARATIVE REVIEW OF DAMAGE AND FAILURE MODELS AND A TABULATED GENERALIZATION

AUTHORS:
P.A. Du Bois[1], S. Kolling[2], M. Feucht[2], A. Haufe[3]

[1] Consulting Engineer, Freiligrathstr. 6, 63071 Offenbach, Germany
[2] DaimlerChrysler AG, EP/SPB, HPC X271, D-71059 Sindelfingen, Germany
[3] Dynamore GmbH, Industriestr. 2, D-70565 Stuttgart, Germany

ABSTRACT:

Reliable prediction of damage and failure in structural parts is a major challenge posed in engineering mechanics. Although solid material models predicting the deformation behaviour of a structure are increasingly available, reliable prediction of failure remains still open.

With SAMP (a Semi-Analytical Model for Polymers), a general and flexible plasticity model is available in LS-DYNA since version 971. Although originally developed for plastics, the plasticity formulation in SAMP is generally applicable to materials that exhibit permanent deformation, such as thermoplastics, crushable foam, soil and metals.

In this paper, we present a generalized damage and failure procedure that has been implemented in SAMP and will be available in LS-DYNA soon. In particular, important effects such as triaxiality, strain rate dependency, regularization and non-proportional loading are considered in SAMP. All required physical material parameters are provided in a user-friendly tabulated way. It is shown that our formalism includes many different damage and failure models as special cases, such as the well-known formulations by Johnson-Cook, Chaboche, Lemaitre and Gurson among others.

Keywords:

Ductile Damage, Failure, Visco-Plasticity, Explicit Finite Element Method

INTRODUCTION

Simulation of failure in shell-like structures is a topic of considerable investigation both in industrial and academic environment alike. The reasons for such a remarkable interest are obviously: very high and ultra high strength steels may exhibit reduced ductility, plastic trim panels fail during side impact and possibility of failure during crash events needs to be considered in numerical simulations. Although the demand on corresponding material formulations is clear, the technology of simulating failure is still in it's infancy.

Before we start, some general aspects of failure simulation should be summarized. First of all, it should be emphasized that the finite element mesh should be fine enough to capture localization arising before failure. Each softening problem is inherently mesh-dependent; no material and/or failure law is meaningful unless it is regularized. A user-friendly way is the so-called crash-regularization [8]. A verification and validation (V&V) process is needed to calibrate a damage and/or failure law to physical experiments. A problem hereby is the physical material data which are needed up to failure. True hardening data beyond necking strain can only be obtained through reverse engineering.

If fracture occurs, a simply connected part must be separated into multiply connected parts. In a Lagrangian description in general and in explicit methods in particular, the most common version of crack simulation is element erosion, i.e. elements are deleted from computation if a certain criterion is fulfilled. The big advantage of this simple procedure is that no new element nodes must be generated which is indispensable in the simulation of "real" crack propagation [4].

Finally, we don't want to conceal that the stress-strain path during manufacturing may influence failure during crash event, i.e. consideration of deformation history is not negligible in general and represents a topic of further investigation for the next years.

Numerous damage models can be found in the literature. Probably the simplest concept is elastic damage where the damage parameter (usually written as d) is a function of the elastic energy and effectively reduces the elastic modulae of the material. In the case of ductile damage, d is a function of plastic straining and affects the yield stress rather than the elastic modulae. This is equivalent to plastic softening. In more sophisticated damage models, d depends on both the plastic straining and the elastic energy (and maybe other factors) and affects yield stress as well as elastic modulae, see [1].

This paper presents a comparison review of the damage and failure models which are implemented in the LS-DYNA package and suggests a generalized formulation for the SAMP-1 model [2], [3]. From a physical point of view, it is instructive to divide the topic into two parts. In the first part, we describe the failure process that occurs when a

failure variable reaches a critical value. In the second part, material strength and/or material stiffness are reduced in function of a damage variable. In most damage models, the damage variable serves as a failure variable simultaneously.

FAILURE MODELS

As failure criteria in LS-DYNA, we can distinguish: principal strain ε_1, thinning ε_3, equivalent plastic strain ε_p, forming limit diagram ε_{fld} and the Johnson-Cook criterion. Some models consider strain-rate dependent failure as well. A very popular failure criterion is given by Johnson and Cook [5]:

$$\varepsilon_f = \left[d_1 + d_2 \exp\left(d_3 \frac{p}{\sigma_{vm}} \right) \right] \left(1 + d_4 \ln \frac{\dot{\varepsilon}}{\dot{\varepsilon}_0} \right), \qquad \text{(Eq. 1)}$$

where d_i are material parameters and the ratio pressure p divided by von Mises stress σ_{vm} is referred to as triaxiality. Figure 1 shows a comparison of different failure models to the Johnson-Cook criterion using Hancock-McKenzie parameters: $d_1 = 0$, $d_2 = \frac{3}{2}$ and $d_3 = \varepsilon_{1f} \exp\left(-\frac{1}{2}\right)$, see [6]. Note that these parameters are tangent to the diffuse necking (FLD) in the neighbourhood of uniaxial stress.

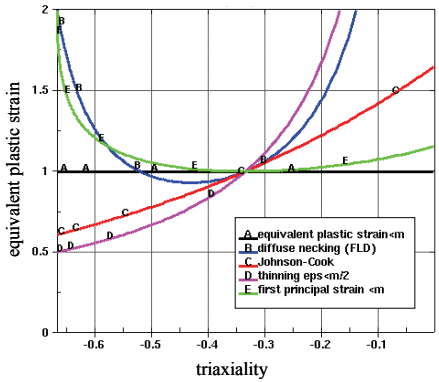

Figure 1: Comparison of different failure models fitted for uniaxial tension

	$a=\sigma_2/\sigma_1$	$b=\varepsilon_{p2}/\varepsilon_{p1}$	p/σ_{vm}
Uniaxial stress Tension	0	-0.5	-0.3333
Biaxial stress	1	1	-0.6666
Uniaxial tension laterally confined	0.5	0	-0.57735
Pure shear	-1	-1	0
Uniaxial stress Compression		-2	0.3333

Table 1: Typical triaxiality values for proportional stress-strain paths

The Johnson-Cook law is implemented as material No. 15 in LS-DYNA. Please note that the strain rate $\dot{\varepsilon}$ in LS-DYNA may be the effective strain rate $\dot{\varepsilon}_{eff}$ or the plastic strain rate $\dot{\varepsilon}_p$ dependent on the optional flag VP. Failure occurs when the accumulated damage value

$$d = \int \frac{d\varepsilon_p}{\varepsilon_f} \leq 1 \qquad \text{(Eq. 2)}$$

reaches the value of 1. This procedure yields to a load path dependent failure and takes non-proportional loading into account.

In contrast to the Johnson-Cook model, our precious MAT_24 considers neither non-proportional loading and triaxiality nor strain rate dependency and is thus not suitable for failure prediction in real structures with complex states of stress. Table 1 gives an overview of some commonly used failure criteria in LS-DYNA.

Law No.	Failure Criterion(s)	Dependency of		
		load path	strain rate	state of stress
MAT_24	$\varepsilon_p \leq \varepsilon_{pf}$ (plastic strain at failure)	yes	no	no
MAT_123	$\varepsilon_p \leq \varepsilon_{pf}$ (plastic strain at failure)	yes	no	no
	$\varepsilon_1 \leq \varepsilon_{1f}$ (major strain at failure)	no	no	no
	$\varepsilon_3 \leq \varepsilon_{3f}$ (thinning)	no	no	no
MAT_15	$d = \int \frac{d\varepsilon_p}{\varepsilon_f} \leq 1$ (accumulation) $\varepsilon_f = \left(d_1 + d_2 e^{d_3 \frac{p}{\sigma_{vm}}} \right) \left(1 + d_4 \ln \frac{\dot{\varepsilon}}{\dot{\varepsilon}_0} \right)$	yes	yes	yes
MAT_39	$\varepsilon_1 \leq \varepsilon_{1fld}(\varepsilon_2)$ (forming limit diagram)	no	no	yes
MAT_81	$\varepsilon_1 \leq \varepsilon_1(\ln \dot{\varepsilon})$	no	yes	no

Table 2: Comparison of some failure models in LS-DYNA

FAILURE MODELS IN SAMP-1

A simple damage model is used in SAMP-1 where the critical damage parameter d_c is a product-function including triaxiality p/σ_{vm}, plastic strain rate $\dot{\varepsilon}$ and element size l_{el} for regularization:

$$d_c = f\left(\frac{p}{\sigma_{vm}}\right)\cdot g\left(\dot{\varepsilon}_p\right)\cdot h\left(l_{el}\right).$$

All functions must be provided by the user as load curves allowing for the flexibility of direct input from test data. The value of the critical damage d_c which leads to rupture is another required additional input. The implemented damage model is isotropic. An evolution law for the failure variable is defined by

$$d = \int \frac{d\varepsilon_p}{f\left(\frac{p}{\sigma_{vm}}\right)\cdot g\left(\dot{\varepsilon}_p\right)} \qquad \text{(Eq. 3)}$$

and failure occurs when $d=d_c$. For proportional loading at constant strain rate the evolution law simplifies to

$$d = \int \frac{d\varepsilon_p}{f\left(\frac{p}{\sigma_{vm}}\right)\cdot g\left(\dot{\varepsilon}_p\right)} = \frac{\varepsilon_p}{f\left(\frac{p}{\sigma_{vm}}\right)\cdot g\left(\dot{\varepsilon}_p\right)} \qquad \text{(Eq. 4)}$$

and thus we may define a critical plastic strain at failure as

$$d \le d_c \Rightarrow \varepsilon_p \le \varepsilon_{pf} = d_c f\left(\frac{p}{\sigma_{vm}}\right)\cdot g\left(\dot{\varepsilon}_p\right) \qquad \text{(Eq. 5)}$$

which reveals the chosen formulation as a generalized Johnson-Cook model.

EXAMPLES

In the following examples we show the influence of triaxiality and non-proportional loading on the failure behaviour. Figures 2 and 3 show the influence of triaxiality where A represents uniaxial stress, B uniaxial strain, C uniaxial strain followed by uniaxial stress and D uniaxial stress followed by uniaxial strain.

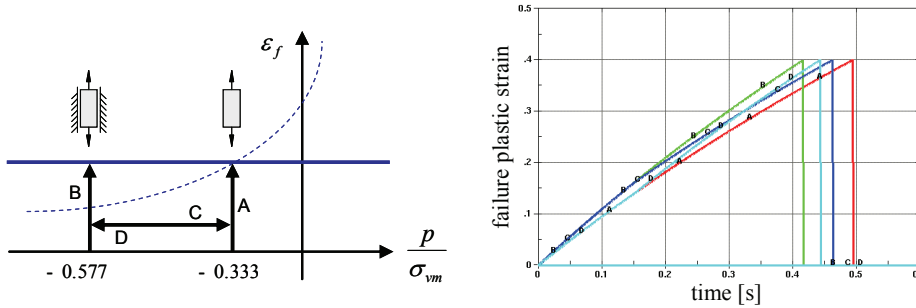

Figure 2: Proportional and non-proportional loading without triaxiality

When no triaxiality is considered (Figure 2), all load cases show the same plastic strain at failure. Because of the different state of stress, however, failure takes place at a various time. Figure 3 shows the influence of triaxiality in detail (we choose same failure conditions under uniaxial tension): load paths A, B, and C fail at the same plastic strain while D fails earlier according to the given curve.

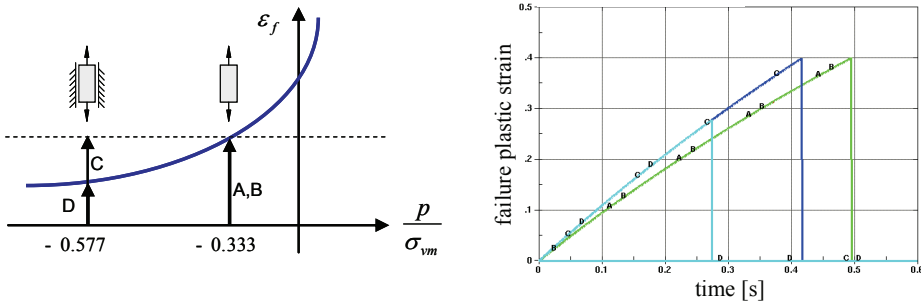

Figure 3: Proportional loading with (A, D) and without triaxiality (B, C)

Figure 4 demonstrates the influence on non-proportional loading. The curves A and B represent proportional loading, C and D represent non-proportional loading where D considers the loading history (accumulation) and C not. Comparison between A and B shows again the known effect on triaxiality. Additionally, the lateral confinement is now lifted in the curves C and D. If the history is taken into account (D), failure takes place at a smaller plastic strain.

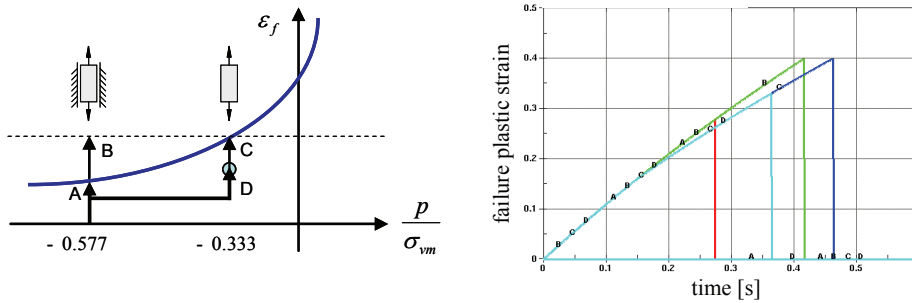

Figure 4: Direct comparison of proportional and non-proportional loading without and with accumulation

DAMAGE MODELS

Damage allows fitting of the unloading path, cyclic loading paths and load paths with strain softening. A damage variable (usually denoted as *d* or *f)* quantifies the part of the material cross section that no longer transmits forces (cracks or voids). In the following, only isotropic damage is considered. Elastic damage effects material stiffness (reduction of elastic modulus). Ductile damage effects material strength (reduction of yield stress) or both material strength and material stiffness. This depends on the chosen formulation where two different approaches may be postulated: strain equivalence or energy equivalence, see table 3.

Formulation	Effective Geometry	Effective Stress	Damaged Modulus
strain equivalence	$A = A_{eff}(1-d)$	$\sigma = \sigma_{eff}(1-d)$	$E_d = E(1-d)$
energy equivalence	$V = V_{eff}(1-f)$	$\sigma = \sigma_{eff}(1-f)\frac{\dot{\varepsilon}_{p,eff}}{\dot{\varepsilon}_p}$	$E_d = E$

Table 3: Strain equivalence and energy equivalence

Strain equivalence effects both yield curve and Young's modulus whereby energy equivalence effects the yield curve only. The latter one is used in the damage model by Gurson [10] and in the extended version of Tvergaard & Needleman [7]. The yield function is defined as

Law No.	Damage Evolution	Path depen-dent	Non-prop. loading
MAT_81	$d = d(\varepsilon_p)$ tabulated	yes	no
MAT_81	$d = \int_{\varepsilon_{pd}}^{\varepsilon_p} d_c \frac{d\varepsilon_p}{\varepsilon_{pr} - \varepsilon_{pd}}$	yes	no
MAT_105	$d = \int_{\varepsilon_{pd}}^{\varepsilon_p} \frac{\sigma_{vm}^2 \left[\frac{3}{2}(1+\nu) + 3(1-2\nu)\left(\frac{\sigma_H}{\sigma_{vm}}\right)^2 \right]}{2E(1-d)^2 S} d\varepsilon_p$	yes	yes
MAT_120	$\dot{f} = (1-f)\dot{\varepsilon}_{vp} + \frac{f_n}{s_n\sqrt{2\pi}} e^{-1/2\left(\frac{\varepsilon_p - \varepsilon_N}{s_N}\right)^2} \dot{\varepsilon}_p$ $f^*(f) = \begin{cases} f & if \quad f < f_c \\ f_c + \frac{1/q_1 - f_c}{f_f - f_c}(f - f_c) & if \quad f > f_c \end{cases}$ $d = q_1 f^*(f) \le d_c = 1$	yes	yes
MAT_187	$d = d(\varepsilon_p)$ tabulated	yes	yes/no

Table 4: Damage models in LS-DYNA

$$\Phi = \frac{\sigma_{vm}^2}{\sigma_{y,eff}^2} + 2q_1 f^* \cosh\left(\frac{q_2 - 3p}{2\sigma_{y,eff}}\right) - 1 - \left(q_1 f^*\right)^2 = 0 \qquad \text{(Eq. 6)}$$

The evolution laws of the damage variables for the different approaches are given in table 4. Figure 5a) shows damage in function of longitudinal plastic strain under uniaxial tension for MAT_81 (A), Gurson (B) and MAT_105 (C, perfect plasticity), compared to Johnson-Cook. Failure plastic strain in function of triaxiality for the damage models by Lemaitre (A) Johnson-Cook (B) and Gurson (D) is plotted in Figure 5b).

a) Damage b) Triaxiality

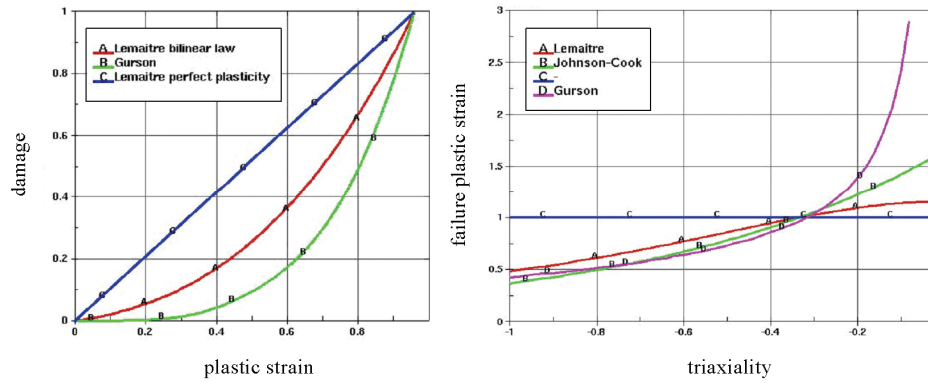

Figure 5: Damage and triaxiality compared to Johnson-Cook

DAMAGE MODELS IN SAMP-1

The model uses the notion of the effective cross section, which is the true cross section of the material minus the cracks that have developed. We define the effective stress as the force divided by the effective cross section

$$\sigma = \frac{F}{A},\ \sigma_{eff} = \frac{F}{A_{eff}} = \frac{F}{A(1-d)} = \frac{\sigma}{1-d} \qquad \text{(Eq. 7)}$$

which allows defining an effective yield stress of $\sigma_{y,eff} = \frac{\sigma_y}{1-d}$. The damaged yield function in SAMP is given by

$$\Phi = \sigma_{vm}^2 - A_2 p^2 - (1-d)A_1 p - (1-d)^2 A_0 \qquad \text{(Eq. 8)}$$

By application of the principle of strain equivalence, stating that if the undamaged modulus is used, the effective stress corresponds to the same elastic strain as the true stress using the damaged modulus, one can write $E = \frac{\sigma_{eff}}{\varepsilon_e}$, $E_d = \frac{\sigma}{\varepsilon_e} = E(1-d)$. Note that the plastic strains are therefore the same: $\varepsilon_p = \varepsilon - \frac{\sigma_{eff}}{E} = \varepsilon - \frac{\sigma}{E_d}$. No damage will occur under pure elastic deformation with this model. Among others, the damage model

represents a good approximation to fit the unloading behavior of plastics [11]. A similar model is given by Lemaitre, where the damaged yield function is given by

$$\Phi = \sigma_{vm}^2 - (1-d)^2 \sigma_{y,eff}^2 \left(\varepsilon_{p,eff}\right) \qquad \text{(Eq. 9)}$$

which leads to the same formulation as SAMP if we set $A_1 = A_2 = 0$ and $A_0 = \sigma_{y,eff}^2$. For a comparison of the chosen model with the formulation by Gurson we may rewrite

$$\Phi = \frac{\sigma_{vm}^2}{\sigma_{y,eff}^2} + 2q_1 f^* \cosh\left(\frac{q_2 - 3p}{2\sigma_{y,eff}}\right) - 1 - \left(q_1 f^*\right)^2 = 0 \qquad \text{(Eq. 10)}$$

With $\cosh(x) \approx 1 + \frac{x^2}{2}$ we obtain a Taylor-approximation of Gurson's yield surface by

$$\Phi \approx \sigma_{vm}^2 + \frac{9}{4} q_1 f^* q_2^2 p^2 - (1 - q1 f*)^2 \sigma_{y,eff}^2 \qquad \text{(Eq. 11)}$$

Comparison with (Eq. 8) yields the SAMP-parameters to be $d = q_1 f^*$, $A_0 = \sigma_{y,eff}^2$, $A_1 = 0$ and $A_2 = -\frac{9}{4} d q_2^2 \neq \text{const}$. Not that the last term is non-constant, i.e. the shape of the yield surface changes with increasing damage, see figure 6.

As a final example, we compare the damage model in SAMP with Gurson's formulation, where Gurson's evolution law is approximated in SAMP by an equivalent tabulated input consisting of damage in function of plastic strain. Figure 7 shows the results for proportional loading like sketched in figure 3.

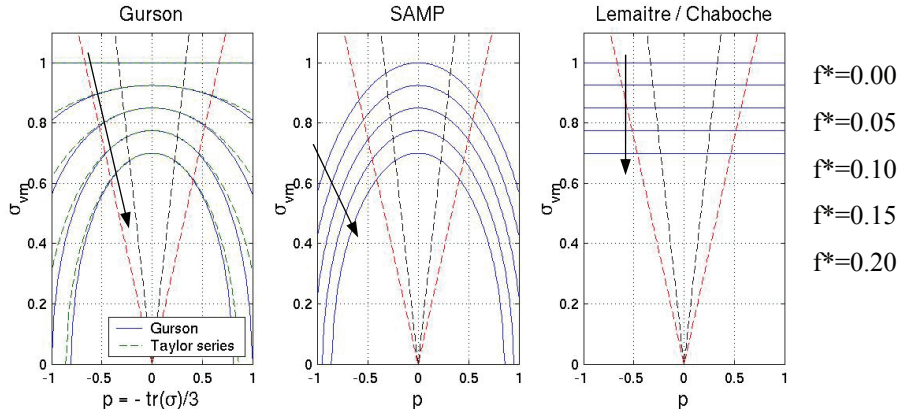

Figure 6: Evolution of the yield surface in function of damage in invariant plane

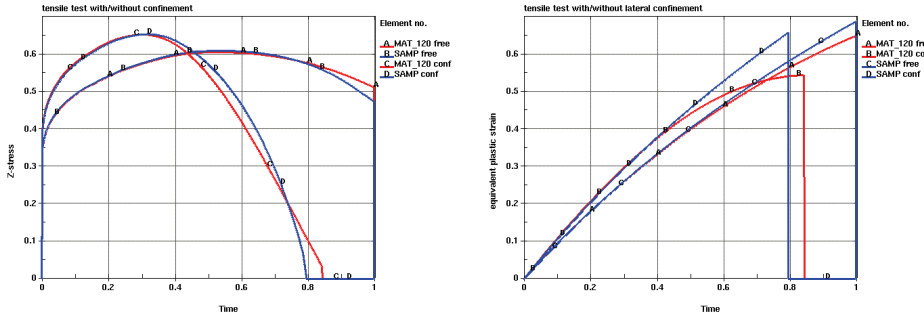

Figure 7: Comparison SAMP - Gurson for proportional loading

As can be seen, SAMP gives a good approximation to the damage/failure model by Gurson. The same is true for non-proportional loading (figure 8) where uniaxial tension changes into lateral confined tension and vice versa. However it should be emphasized that SAMP is not equivalent to the Gurson model but is able to lead to comparable results.

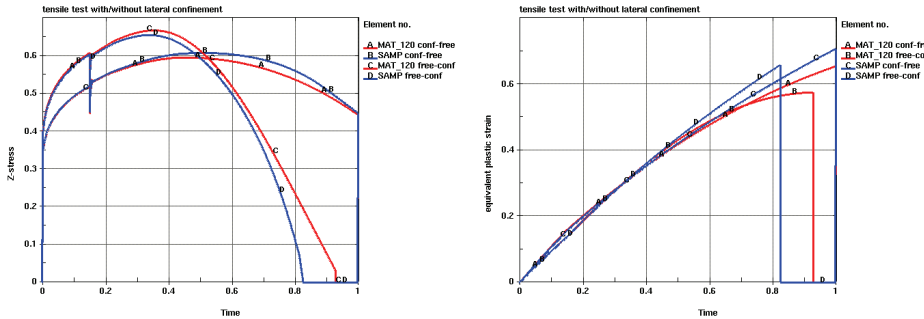

Figure 8: Comparison SAMP - Gurson for non-proportional loading

SUMMARY AND CONCLUSIONS

A tabulated failure formulation has been added to the SAMP material model. This encapsulates many previously implemented formulations (e.g. FLD, Johnson-Cook) as long as the failure variable depends on plastic strain. Hereby, the failure variable can be total or incremental (accumulated). Furthermore, a generalized damage formulation has been implemented for SAMP where the input is fully tabulated. Existing damage models can largely be recovered (e.g. Lemaitre, Chaboche and Gurson among others). This model allows for a considerable flexibility to fit experimental data from tests with

unloading or failure. The presented failure formulation and damage model will be implemented in MAT_187 next.

REFERENCES

[1] Lemaitre, J.; Chaboche, J.-L. (1988): Mécanique des matériaux solides, Dunod.

[2] Kolling, S; Haufe, A.; Feucht, M; Du Bois, P.A. (2006): A constitutive formulation for polymers subjected to high strain rates. Proceedings of the 9th International LS-DYNA Users Conference, Dearborn, Michigan, USA, **15**: 55-74.

[3] Du Bois, P.A.; Haufe, A.; Feucht, M.; Kolling, S. (2006): A generalized damage and failure formulation for SAMP. Proceedings of the 5th German LS-DYNA Forum, Ulm, Germany, **A-II**: 77-110.

[4] Baaser, H.; Gross, D. (2001): 3D nonlocal simulation of ductile crack growth - a numerical realization. European Journal of Finite Elements **10** (2-3-4): 353-367.

[5] Johnson, G.R.; Cook, W.H. (1983): A constitutive model and data for metals subjected to large strains, high strain rates and high temperatures. Proceedings of the 7th International Symposium on Ballistics, The Hague, Netherlands, pp. 541-547.

[6] Hancock, J.W.; Mackenzie, A.C. (1976): On the mechanics of ductile failure in high-strength steel subjected to multi-axial stress-states, Journal of Mechanics and Physics of Solids **24**: 147-169.

[7] Needleman, A.; Tvergaard, V., (1984): Analysis of Ductile Rupture in Notched Bars. J. Mech. Phys. Solids **32**, pp. 461-490.

[8] Feucht, M.; Faßnacht, W. (1999): Simulation der duktilen Rissbildung in Crashberechnungen mit Hilfe des Gurson-Modells. 17. CADFEM User's meeting, III-4.3, Sonthofen.

[9] Feucht, M. (2004): Regularized Damage Modelling for Failure Prediction of Automotive Components under Crash Loading. In Proceedings of 5th International Conference of Computation of Shells and Spatial Structures, Salzburg, Austria.

[10] Gurson, A.L. (1977): Continuum theory of Ductile Rupture by Void Nucleation and Growth; Part 1-Yield Criteria and Flow Rules for porous Ductile Media. J. Eng. Mater. Tech. **99**, 2-15.

[11] Du Bois, P.A.; Kolling, S.; Koesters, M.; Frank, T.(2006): Material behavior of polymers under impact loading. International Journal of Impact Engineering, **32**: 725-740.